JPE

A New Soft Switching Dual Input Converter for Renewable Energy Systems

Amir Torki Harchegani† and Mohammad Mahdavi*

†*Department of Electrical Engineering, Isfahan (Khorasgan) Branch, Islamic Azad University, Isfahan, Iran

Abstract

This paper proposes a new soft switching dual input converter for renewable energy systems. Multi-input converters are produced by combining discrete converters. These converters reduce the number of circuit elements, cost, volume and weight of the converter and provide a constant output power in different weather conditions. Furthermore, soft switching techniques can be applied to increase efficiency. In this paper, a Zero Voltage Transition (ZVT) dual input boost converter is presented. Only one auxiliary circuit is used to provide the soft switching condition for all of the semiconductor elements. The proposed converter, which is simulated by ORCAD software, is theoretically analyzed. To confirm the validity of the theoretical analysis, a prototype of proposed converter was constructed. Simulation and experimental results confirm the theoretical analysis. An efficiency comparison shows a one percent improvement at nominal loads.

Key words: Multi Input Converter (MIC), renewable energy systems, soft switching, ZVT, boost

I. INTRODUCTION

In the last decade, the use of renewable energy sources has rapidly increased due to fossil fuel crisis, global warming and environmental pollution. Due to the Kyoto Protocol, clean energies including fuel cells, Photovoltaics, wind energy, etc. have been quickly promoted [1]-[7]. Photovoltaics and wind energy have the ability to supply the demand energy, even in remote or off grid places and in densely populated areas. Since obtaining power from renewable energy sources depends on environmental conditions such as different seasons and climate, the concurrent use of these resources is inevitable to ensure a continuous supply energy [8]. Although the multi-input structure was first proposed in 1999, it has a scientifically traditional background. The count of passive elements and the cost semiconductor elements can be reduced by using a multi-input converter (MIC). For example, as a result of using a single output filter for several converters, the size and losses of these converters is decreased. The Possibility of easier control, higher flexibility and better management of energy sources are other advantages of MICs.

MICs fall in two categories including Electrically Coupled Converters (ECCs) and Magnetically Coupled Converters (MCCs) [9]-[17]. ECCs have both advantages and disadvantages. Some of the advantages are easier control in the presence of a variable input and high reliability when compared to MCCs. The disadvantages include non-isolation between the input and output and non-multilevel outputs.

The main goal of researchers has been to improve the efficiency and reliability, and reduce the cost of systems. Therefore, different soft switching techniques have been proposed in the literature to improve the efficiency of switching converters [18]-[27]. These soft switching techniques also reduce Electromagnetic Interference (EMI) by lowering dv/dt and di/dt; while decreasing the switching losses.

The authors of [28], [29] sought to provide the soft switching condition and enhance the efficiency of multi input converters by adding one auxiliary circuit. A major problem of these topologies is to provide the soft switching condition for main switches while the auxiliary switch is switched under the hard switching condition.

In this paper, a soft switching dual input converter for the simultaneous or independent use of solar and wind energy is proposed. The proposed converter simultaneously provides soft switching for all of the semiconductor elements with only one auxiliary circuit. It also solves the above mentioned problems and provides soft switching condition for all forms of semiconductor elements.

In section II the theoretical performance of the presented converter is investigated. Section III covers the design

considerations. Section IV describes the design of the proposed converter with a 400W output power which is then simulated by the ORCAD software. Then in section V, a prototype of the proposed converter is built. Experimental results are obtained and then compared with the theoretical analysis. Finally, some conclusions are presented in section VI.

II. PROPOSED CONVERTER

Fig. 1 shows the proposed soft switching dual input converter. The proposed converter consists of two combined boost converters with one auxiliary cell that provides the ZVS condition for all of the semiconductor elements. The auxiliary circuit is illustrated in the dotted box. The presented converter can work with two input sources simultaneously or with one source independently.

The following assumptions are considered to analyze the presented converter in the steady state operation and during a switching cycle. The input inductors (L_{m1}, L_{m2}) and the output capacitor C_o are assumed to be large enough that these elements can be considered as an ideal DC current and voltage source, respectively. All of the circuit elements are considered to be ideal and the converter operates in the Continuous Conducting Mode (CCM).

Based on the above assumptions, fig. 2 shows an equivalent circuit model of the proposed converter. The operation of this converter is analyzed in nine modes. It should be noted that the two main switches are turned on at the same time. However, they can be asynchronously turned off. Fig. 4 shows an equivalent circuit model of each mode. Key waveforms of the theoretical analysis are shown in fig. 3. It is assumed that before the first mode, all of the semiconductor devices are off except for D_1 and D_2. In addition, the voltage of C_{r1} and C_{r2} and the current of L_r are zero.

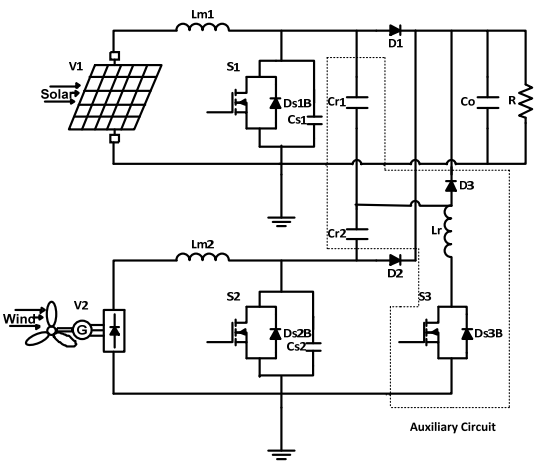

Fig. 1. Proposed ZVT dual input converter.

The converter analysis is given in two states. It is assumed that the input currents are equals in the first state and not equal in the second state and that $I_{in1}<I_{in2}$.

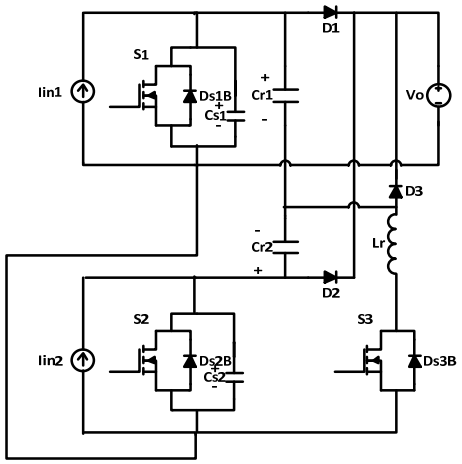

Fig. 2. Equivalent circuit model of the proposed ZVT dual input converter.

A. Equal input currents ($I_{in1}=I_{in2}$)

Mode 1 [t_0-t_1]: At the beginning of this mode the auxiliary switch S_3 is turned on. Therefore, a resonance occurs between L_r, C_{r1} and C_{r2}, and the L_r current resonantly increases from zero. Thus, the ZC condition is provided for S_3. This mode lasts until the current of L_r reaches $2I_{in1}$. Thus, the L_r current and the C_r voltage are calculated as follows:

$$I_{lr} = \frac{V_o}{Z_1}\sin(\omega_1(t-t_0)) \quad (1)$$

$$V_{cr}(t) = V_o - V_o\cos(\omega_1(t-t_0)) \quad (2)$$

Where: $Z_1 = \sqrt{\frac{L_r}{C_r}}$, $C_r = C_{r1} + C_{r2}$, $\omega_1 = \frac{1}{\sqrt{L_r C_r}}$

Therefore, the duration of this mode and $V_{Cr}(t_1)$ are:

$$t_1 - t_0 = \frac{\sin^{-1}\frac{2I_{in1}Z_1}{V_o}}{\omega_1} \quad (3)$$

$$V_{Cr}(t_1) = V_O - \sqrt{V_O^2 - 4Z_1^2 I_{in1}^2} \quad (4)$$

Mode 2 [t_1-t_2]: By reaching the L_r current to $2I_{in1}$, this mode is started. Therefore, D_1 and D_2 are turned off under the ZVZC condition. Then a resonance occurs between Lr, C_{r1}, C_{r2}, C_{S1} and C_{S2}. This mode continues until the switch voltage reaches zero. The current of L_r and the voltage of C_r and C_S can be calculated as follows:

$$I_{Lr}(t) = \frac{V_1}{Z_2}\sin(\omega_2(t-t_1)) + \frac{C}{C_r}2I_{in1}\cos(\omega_2(t-t_1)) + \frac{C}{C_s}2I_{in1} \quad (5)$$

$$V_{Cs}(t) = \frac{C}{C_s}[V_1\cos(\omega_2(t-t_1)) - \frac{C}{C_r}I_{in}Z_2 * \sin(\omega_2(t-t_1)) - V_1] + \frac{2I_{in1}C}{C_s^2}(t-t_1) + V_O \quad (6)$$

$$I_{Lrp} = \sqrt{\frac{V_1^2 + (2I_{in1}Z_2)^2}{Z_2}} + \frac{C}{C_s}2I_{in1} \quad (7)$$

$$V_{Cr}(t) = \frac{C}{C_r}[V_1\cos(\omega_2 (t - t_1)) - \frac{C}{C_r} 2I_{in1} Z_2 \sin(\omega_2 (t - t_1)) - V_1] + \frac{2I_{in1}C}{C_r C_s}(t - t_1) + V_{Cr}(t_1) \quad (8)$$

Where:

$$C_S = C_{s1} + C_{s2} \quad , \quad C = \frac{C_r C_s}{C_r + C_s} \quad , \quad V_1 = V_O - V_{Cr}(t_1) \quad ,$$

$$Z_2 = \sqrt{\frac{L_r}{C}} = \sqrt{\frac{L_r (C_r + C_s)}{C_s C_r}} \quad , \quad \omega_2 = \frac{1}{\sqrt{L_r C}} = \sqrt{\frac{(C_r + C_s)}{L_r C_s C_r}}$$

Mode 3 [t_2-t_3]: When C_s is completely discharged, the body diode of S_1 and S_2 are turned on and this mode is started. It should be mentioned that S_1 and S_2 should be turned on under the zero voltage and zero current (ZVZC) condition. It should also be mentioned that S_1 and S_2 should be turned on before turning off the body diode of the main switches (D_{s1B} and D_{s2B}). I_{Lr} and V_{Cr} are expressed as follows:

$$I_{Lr}(t) = I_2 \cos(\omega_1 (t - t_2)) - \frac{V_2}{Z_1} \sin(\omega_1 (t - t_2)) \quad (9)$$

$$V_{Cr}(t) = V_2 \cos(\omega_1 (t - t_2)) + I_2 Z_1 \sin(\omega_1 (t - t_2)) \quad (10)$$

Where: $I_2 = I_{Lr}(t_2)$, $V_2 = V_{Cr}(t_2) = \frac{I_{in}}{C_r}(t_2 - t_1) + \frac{C_s}{C_r} V_o + V_{Cr}(t_1)$

Mode 4 [t_3-t_4]: When I_{S2} and I_{S1} are increased to I_{in2} and I_{in1}, this mode is started and the body diode of S_3 (D_{s3B}) is turned on. As a result, the auxiliary switch S_3 can be turned off under the ZVZC condition. I_{Lr} reaches zero and the voltage of C_r becomes $V_{cr,P}$. Voltage stress of D_3 is equal to $V_o + V_{cr,P}$. Thus, $V_{cr,P}$ is calculated by (11). The resonance between C_r and L_r continues through the switches S_1, S_2 and D_{s3B}. The maximum current of the S_1 main switch is also expressed by the following equation:

$$V_{Crp} = \sqrt{\frac{L_r I_{Lr}(t_2)^2 + C_r V_{Cr}(t_2)^2}{C_r}} \quad (11)$$

$$I_{s1,p} = I_{in} + I_{Lr,p} \quad (12)$$

Mode 5 [t_4-t_5]: The resonance ends when the S_3 body diode turns off, and this mode is started. This mode is similar to the input inductor charging mode in a conventional boost converter. The input inductors (L_{m1}, L_{m2}) are charged in this mode.

Mode 6 [t_5-t_6]: By turning off S_2, V_{cs2} which is equal to the S_2 switch voltage is linearly charged by the slope of I_{in2}/C_{eq}. Therefore, S_2 is turned off under the ZVS condition. This mode continues until C_{r2} is completely discharged. C_{s2} and C_{r1} are also charged to reach V_O.

$$V_{cs2} = \frac{(t_6 - t_5)}{C_{eq}} I_{in2} \quad (13)$$

Where: $C_{eq} = C_{s2} + \frac{C_{r1} C_{r2}}{C_{r1} + C_{r2}}$

Mode 7 [t_6-t_7]: When V_{cs2} reaches V_O, D_2 turns on at t_6. Therefore, power from the second input is transferred to the output through D_2 while the first input inductor (L_{m1}) is charging.

Mode 8 [t_7-t_8]: By turning off S_1, V_{cs1} which is equal to the switch voltage is charged and C_{r1} is discharged linearly by slope of $I_{in1}/(C_{s1}+C_{r1})$ through D_3. Therefore, D_3 is turned on under the ZV condition. This mode lasts until C_{r1} is completely discharged and C_{s1} is completely charged.

Mode 9 [t_8-t_9]: When C_{r1} is discharged completely, D_1 is turned on. This mode is similar to the power transfer mode to the output in a conventional boost converter. This mode continues until the next switching cycle.

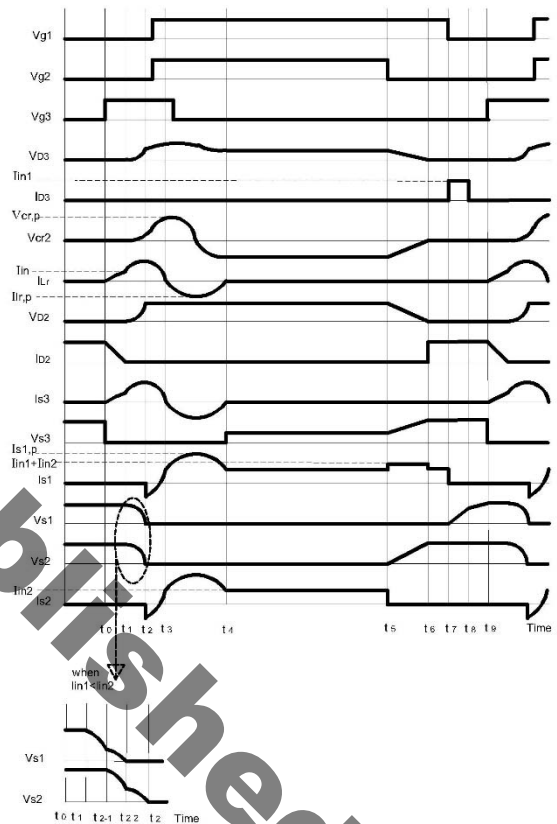

Fig.3. Key waveforms of the proposed converter.

B. Unequal input currents (I_{in1}<I_{in2})

Assuming that I_{in1} is smaller than I_{in2}, only mode 2 is changed by the following modes. The equivalent circuit of the following modes is shown in fig. 5. In order to simplify the equations, it is assumed that C_{r1} and C_{r2} are a lot greater than C_{S1} and C_{S2} in these three modes.

Mode 2.1 [t_1-$t_{2.1}$]: When the C_{r1} current reaches I_{in1}, this mode is started. Therefore, D_1 is turned off under the ZVZC condition. Then the C_{s1} capacitor subsequently starts discharging. A resonance occurs between L_r, C_{r1}, C_{r2} and C_{s1}. This mode lasts until the C_{r2} currents reaches I_{in2}, and D_2 turns off. Therefore:

$$I_{Cr2}(t) = \sqrt{{I_{in1}}^2 + \left(\frac{V_1}{\sqrt{2}Z_1}\right)^2}\sin(\sqrt{2}\omega_1(t - t_1) + \tan^{-1}(\frac{I_{in1}\sqrt{2}Z_1}{V_1})) \quad (14)$$

The duration of this mode can be calculated by $I_{Cr2}(t)=I_{in2}$. Therefore:

$$t_{2.1} - t_1 = (\sin^{-1}\left(\frac{I_{in2}}{\sqrt{{I_{in1}}^2 + \left(\frac{V_1}{\sqrt{2}Z_1}\right)^2}}\right) - \tan^{-1}(\frac{I_{in1}\sqrt{2}Z_1}{V_1}))/\sqrt{2}\omega_1 \quad (15)$$

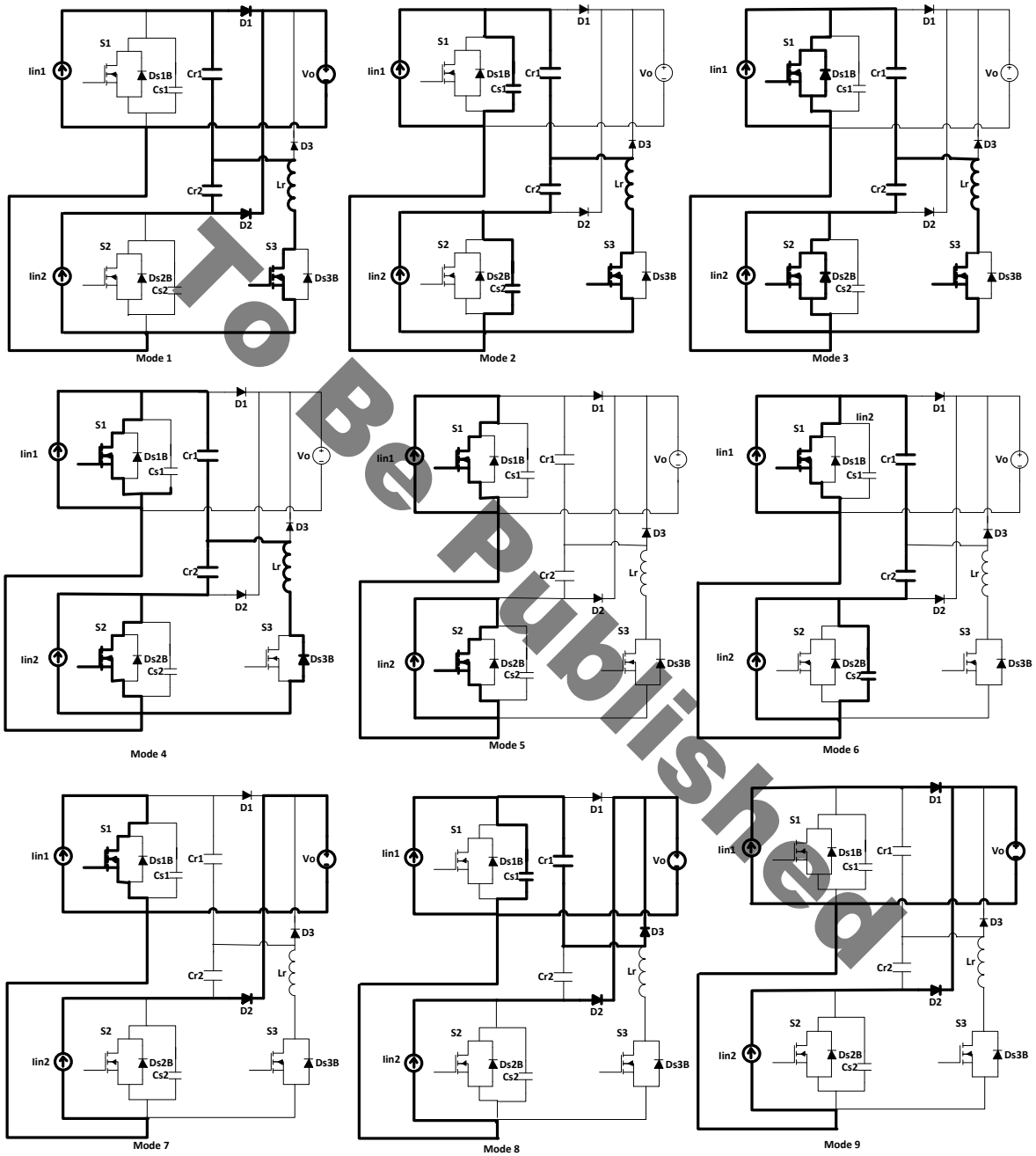

Fig.4. Equivalent circuit models of each mode.

Mode 2.2 [$t_{2.1}$-$t_{2.2}$]: D_2 turns off and C_{s2} starts to discharge through the C_{r2} current reaching I_{in2}. A resonance occurs between L_r, C_{r1}, C_{r2}, C_{s2} and C_{s1}. This mode lasts until C_{s1} is fully discharged, and the body diode of the S_1 switch turns on.

$$V_{Cs1}(t) = A\cos(\frac{\omega_1}{\sqrt{2}}(t - t_{2.1})) + I_{in}\frac{Z_1}{\sqrt{2}}\sin(\frac{\omega_1}{\sqrt{2}}(t - t_{2.1})) + D \quad (16)$$

where: $A = V_O - V_{Cr2}(t_{2.1}) + L_r I_{Lr}(t_{2.1})$,

$D = V_{Cr1}(t_{2.1}) - L_r I_{Lr}(t_{2.1})$, $I_{in} = I_{in1} + I_{in2}$

Mode 2.3 [$t_{2.2}$-t_2]: This mode is started by turning on the

body diode of S_1. The resonant between L_r, C_{r1}, C_{r2} and C_{s2} continues until C_{s2} fully discharges and the body diode of the S_2 switch turns on. At the end of this mode, mode 3 is started and all of the other modes are not changed.

$$V_{Cs1}(t) = E\cos(\sqrt{2}\omega_1(t - t_{2.2})) + F\sin(\sqrt{2}\omega_1(t - t_{2.2})) + G \quad (17)$$

Where:

$$E = V_{Cs2}(t_{2.2}) - V_{Cr2}(t_{2.2}) \quad , \quad F = \sqrt{2}Z_1(I_{in2} - I_{Lr}(t_{2.1})) \quad , \quad G = V_{Cr2}(t_{2.2})$$

EFFICIENCY IMPROVEMENT:

In this section the efficiency improvement is theoretically analyzed. The proposed converter has lower switching losses than its hard switching counterpart due to soft switching. Moreover, the total conduction losses increase through the auxiliary circuit. In order to calculate the total efficiency improvement, these two sources of losses are calculated as follows:

$$P_{Loss,turnon} = 2 \times \frac{1}{2} C_s V_{sw}^2 f_{sw} \quad (18)$$

$$P_{Loss,turnoff} \approx 2 \times \frac{1}{8} V_{sw} I_{sw} t_{off} f_{sw} \quad (19)$$

$$P_{Loss,conduction} = R_{ON} I_{sw3,RMS}^2 T_r / T_{sw} \quad (20)$$

Where V_{sw}, I_{sw}, $I_{sw3,RMS}$ and C_{snb} are the maximum voltage of main switch, the maximum current of the main switch, the RMS current of the auxiliary switch, and the snubber capacitor value in the hard switching counterpart, respectively. Therefore, the total reduction of the converter losses is equal to:

$$P_{improve} = P_{Loss,turnoff} + P_{Loss,turnon} - P_{Loss,conduction} \quad (21)$$

As a result, the percentage of the efficiency improvement is equal to $P_{improve}/P_{out}*100$.

For the design example in the next section:

$$P_{improve} = 3.5 + 4 - 1.7 = 5.8W \quad (22)$$

Thus, the efficiency improvement is about 1.45 percent at the nominal load.

III. DESIGN CONSIDERATION

The design considerations of the proposed converter are explained in four steps.

A. Main element design

Based on the operation mentioned in the previous section, the auxiliary circuit only works at the switching turn off and on instants. Therefore, designing the main elements of the proposed converter (L_{m1}, L_{m2} and C_O) is similar to that of conventional boost converters [30].

B. Auxiliary circuit design

In this section, the design considerations for selecting the resonant or auxiliary circuit elements (C_{r1}, C_{r2}, C_{s1}, C_{s2} and L_r) are presented. C_{s1} and C_{s2} are designed like the snubber capacitor by the following equation:

$$C_{s1}, C_{s2} \geq \frac{I_{in1,2} t_f}{2V_O} \quad (23)$$

Where t_f is the switch fall time.

Based on the converter operation in the second mode, to provide the ZVS condition, C_s should be completely discharged. Therefore, C_r should be selected much higher than C_s. For the design example in the next section, it is assumed that C_r=15C_s.

Base on the converter operation in the first mode, to provide the soft switching condition, the resonant current should reach $2I_{in1}$. Therefore, the following condition should be satisfied:

$$I_{Lr} > 2I_{in1}, \ \frac{V_o}{Z_1} > 2I_{in1} \Rightarrow Z_1 < \frac{V_o}{2I_{in1}} \quad (24)$$

In the worst case, in mode 2.1, C_{r2} current should also reach I_{in2}. For this reason, substituting Equ. (4) in (14) yields:

$$Z_1 < \frac{V_O}{\sqrt{2(I_{in1}^2 + I_{in2}^2)}} \quad (25)$$

To provide the soft switching condition in mode 2.2 and 2.3, the following condition should be satisfied to completely discharge C_{s1} and C_{s2}.

$$Z_1 < \frac{\sqrt{2}(D^2 - A^2)}{I_{in}} \quad (26)$$

Therefore, by selecting Z_1, L_r can be calculated by the following equation:

$$L_r = Z_1^2 C_r \quad (27)$$

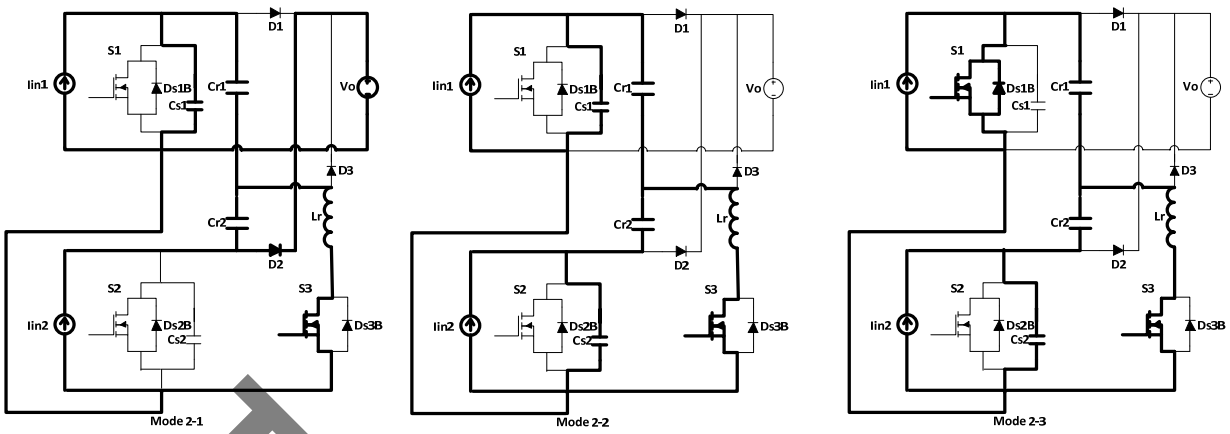

Fig.5. Key waveforms of the proposed converter.

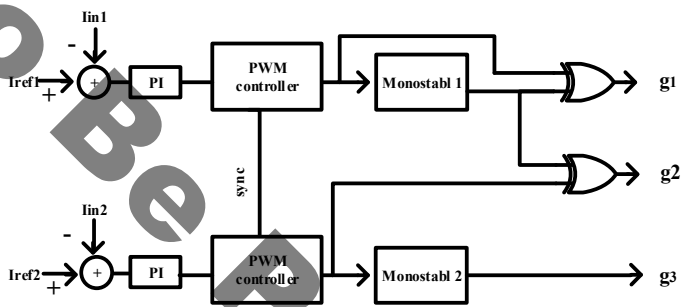

Fig.6. Controller block diagram.

C. Semiconductor elements selection

The design of the semiconductor elements is based on its maximum voltage and current. Therefore:

$$I_{s1} = I_{in1} + I_{Lr,p}\ ,\quad I_{s2} = I_{in2} + I_{Lr,p} \tag{28}$$

$$I_{s3} = I_{Lr,p}\ ,\quad I_{D1} = I_{D3} = I_{in1},\quad I_{D2} = I_{in2} \tag{29}$$

$$V_{s1} = V_{s2} = V_{D1} = V_{D2} = V_o \tag{30}$$

$$V_{s3} = V_{D3} = V_o + V_{Cr,p} \tag{31}$$

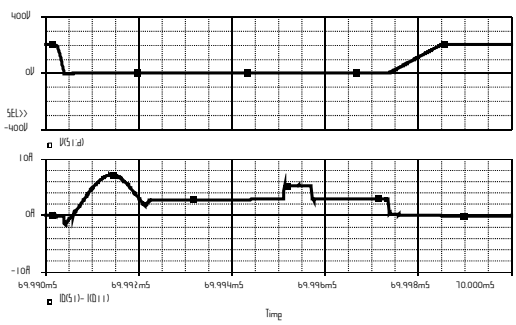

a

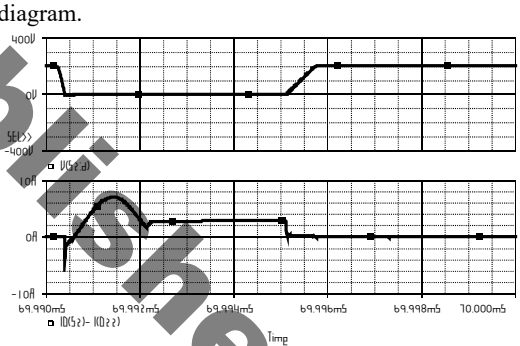

b

Fig.7. Voltage and current waveforms: a) main switch S_1; b) main switch S_2.

D. Controller Circuit

As shown in Fig. 6, the controller circuit of this converter is similar to the conventional PWM controller fully discussed in [31]. It should be noted that only two monostables and two XOR gates should be added to the conventional controller to produce the auxiliary switch gate signal. Furthermore, the two PWM controllers should be synchronized because the main switches are simultaneously turned on. Based on the circuit operation, the pulse width of monostable 1 should be t_2-t_0, which it is about $0.25T_r$; and the pulse width of monostable 2 should be t_3-t_0, which it is about $0.75T_r$.

IV. SIMULATION RESULTS

The presented dual input converter has been designed based on the previous section under the following conditions. Input voltage V_{in1}=50V_{DC}, V_{in2}=100 V_{DC}, output power = 400 Watt, output voltage = 200 V_{DC} and the switching frequency (fs) is 100 KHz.

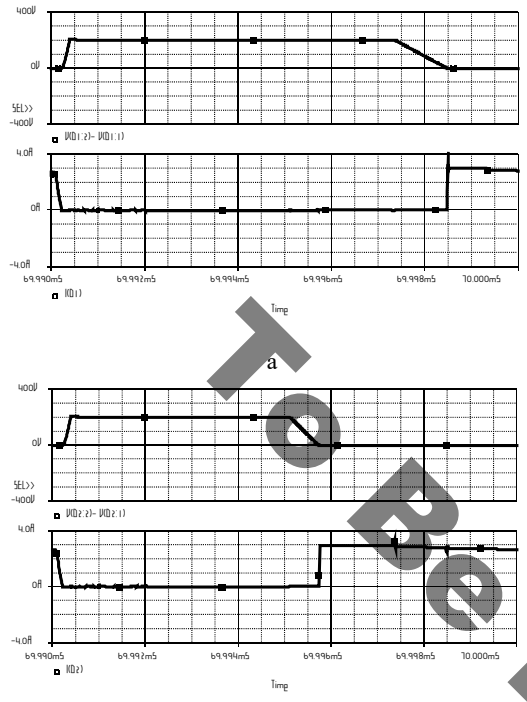

a

b

Fig.8. Voltage and current waveforms: a) main diode D_1; b) main diode D_2.

Therefore, the following circuit elements values are selected L_r=5uH, L_{m1}=L_{m2}=1mH, C_{r1}=C_{r2}=15nF, C_{s1}=C_{s2}=1nF and C_o=100uF. Then the presented dual input converter is simulated by ORCAD software under three conditions. The first condition is when input currents are equal. The second condition is when I_{in1}=0 and I_{in2}=max. The third condition is when I_{in1}=max and I_{in2}=0.

Fig. 7-10 show simulated waveforms of the proposed converter. In all of the simulation results, the upper waveforms are voltages and the lower waveforms are the currents. Fig. 7 a and b show that the main switches turn on under the ZVZC and turn off under the ZV condition.

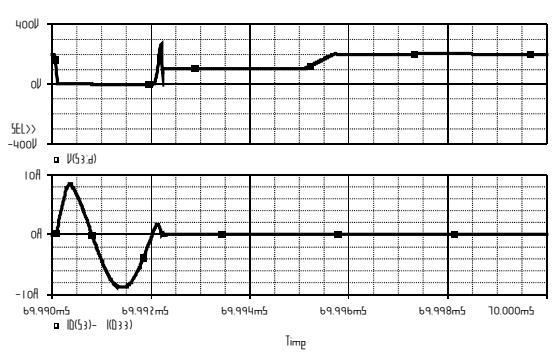

Fig.9. Voltage and current waveforms of the auxiliary switch.

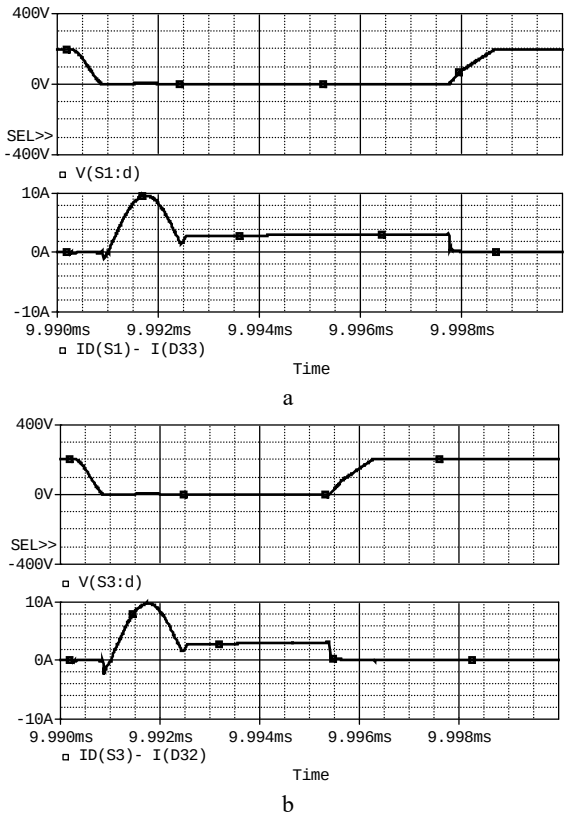

Fig.10. a) Voltage and current waveform: a) main switch S_1, when I_{in2}=0; b) main switch S_2, when I_{in1}=0.

The ZVS conditions for the main diodes are also shown in Fig. 8 a and b. It can be seen from Fig. 9 that the auxiliary switch turns off under the ZVZC and turns on under the ZC condition. Moreover, it shows that the auxiliary switch turns on near the ZCS condition due to the discharging of the parasitic drain-source capacitor. It is obvious that the obtained waveforms confirm the theoretical analysis.

To show that the inputs of the proposed multi input converter can work independently, the proposed converter is simulated under two conditions. In the first condition, the duty cycle of S_2 is zero. In the second condition, the converter operates at the nominal current. As shown in Fig. 10 a, the soft switching condition is provided for S_1. Furthermore, in Fig. 10 b, the duty cycle of S_1 is zero, and the soft switching condition is provided for S_2.

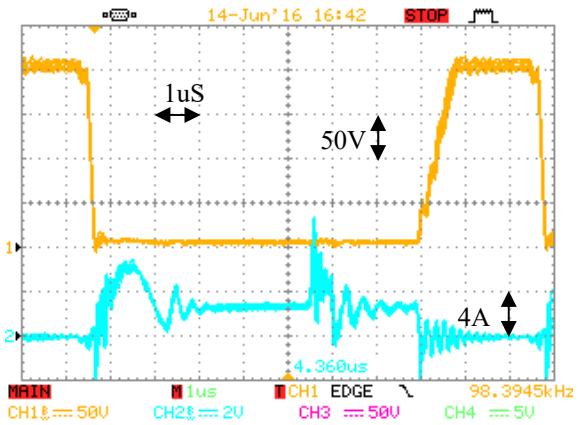

a

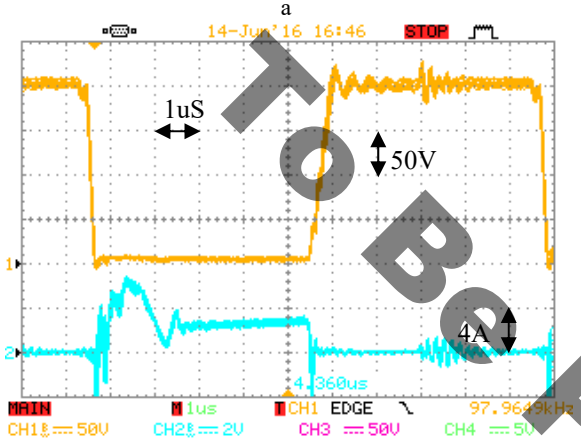

b

Fig.11. Voltage and current waveforms: a) main switch S_1; b) main switch S_2.

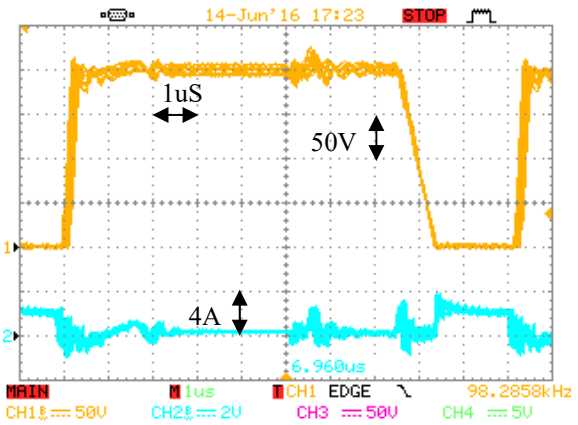

a

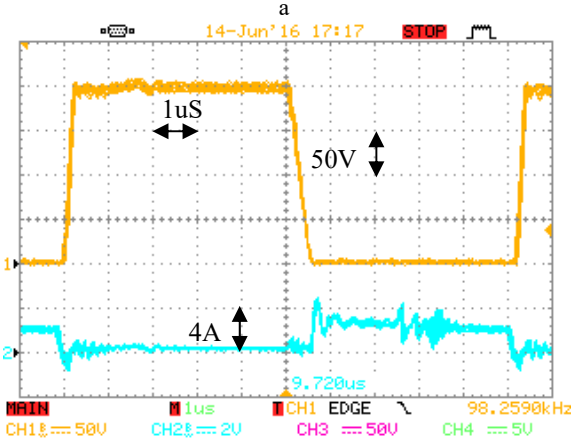

b

Fig.12. Voltage and current waveforms: a) main diode D_1; b) main diode D_2.

V. EXPERIMENTAL RESULTS

To verify the feasibility, a 400W prototype of the simulated converter in the previous section has been constructed. All of the switches, diodes, and auxiliary diode are IRFP460, BYV32 and MUR860, respectively.

The experimental results for the proposed dual input converter are presented in this section. Fig. 11 shows that the main switches turn on under the ZVZC, and turn off under the ZV condition. Fig. 12 shows the zero voltage condition of the main diodes. Fig. 12 also shows that the auxiliary switch turns off under the ZVZC, and turns on under the ZC condition.

The experimental results confirm the validity of the simulation and theoretical analysis. However, there is some ringing in the current waveforms. This is different from the simulation and theoretical analysis. This ringing is due to a resonance between the parasitic capacitors and the inductors. Fig. 13 is the same as the simulation results, except for a resonance during the turn off instant. This is due to a resonance between the resonant inductor and the auxiliary output capacitor. A method for clamping the voltage across the auxiliary switch S_3 is shown in Fig. 14 by adding an extra diode D_4.

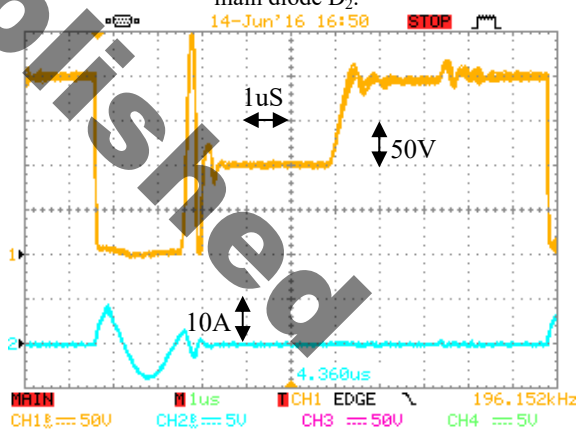

Fig.13. Voltage and current waveforms of the auxiliary switch.

Fig. 15 shows a measured efficiency comparison of the proposed dual input converter and its hard switching counterpart. The efficiency curve is plotted by using experimental results obtained from the laboratory setup. The continuous line shows the efficiency of the proposed dual input converter and the discrete line shows the efficiency of the dual input hard switching converter. This figure shows approximately a one percent improvement in the efficiency of the proposed converter in comparison with its hard switching counterpart. The measured efficiency improvement is lower

than the one percent calculated in section II because the losses are not considered such as the conduction losses of the unwanted resonant, etc.

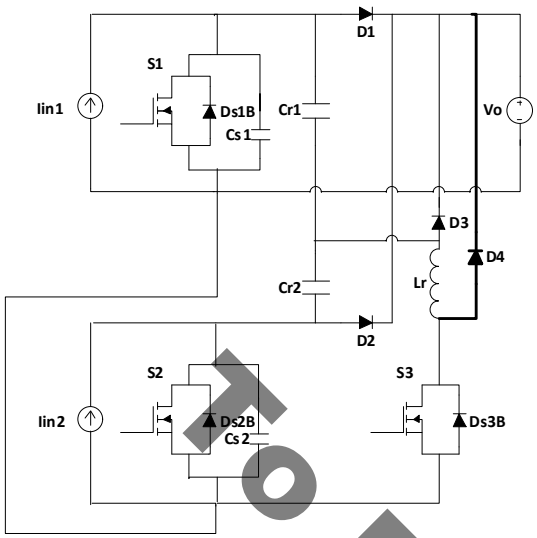

Fig.14. Proposed method for clamping the auxiliary switch voltage S_3.

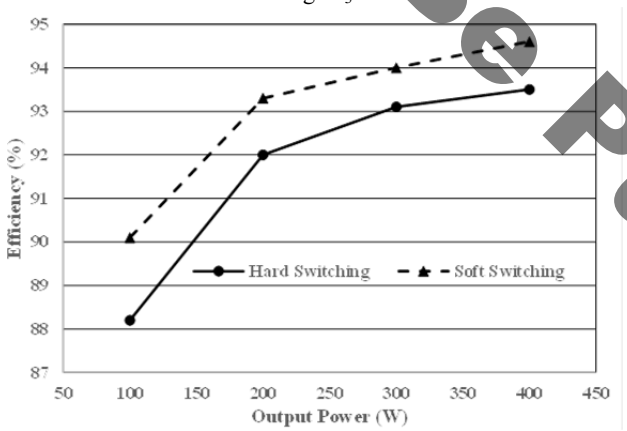

Fig.15. Measured efficiency comparison of the proposed converter and a dual input hard switching boost converter.

VI. CONCLUSIONS

In this paper, a new ZVS dual input converter is proposed. It provides the soft switching condition for all of the semiconductor elements. It is theoretically analyzed and various operating modes, simulation results and experimental results are investigated. Simulation results indicate that the proposed technique can achieve a one percent improvement in the efficiency of the proposed converter at the nominal load. In addition, due to using the ZVT technique, EMI noise can be reduced by decreasing the dv/dt and di/dt. Simulation and experimental results confirm the theoretical analysis. The control of this converter is PWM and the number of required switches to provide the soft switching condition is just one. The diode reverse-recovery problem is improved by providing the ZVS condition for the main diodes. The proposed dual input converter provides soft switching conditions with one auxiliary circuit for all of the semiconductor elements. The proposed idea can be easily expanded for more boost converters, which is one of the strong points of this technique.

REFERENCES

[1] Authors have a responsibility of editing reference list C. L. Shen and P. C. Chiu, "Buck-boost-flyback integrated converter with single switch to achieve high voltage gain for PV or fuel-cell applications," in IET Power Electronics, vol. 9, no. 6, pp. 1228-1237, 5 18 2016.

[2] J. T. Bialasiewicz, "Renewable Energy Systems With Photovoltaic Power Generators: Operation and Modeling," in IEEE Transactions on Industrial Electronics, vol. 55, no. 7, pp. 2752-2758, July 2008.

[3] Y. C. Liu and Y. M. Chen, "A Systematic Approach to Synthesizing Multi-Input DC–DC Converters," in IEEE Transactions on Power Electronics, vol. 24, no. 1, pp. 116-127, Jan. 2009.

[4] L. Wang, Z. Wang and R. Yang, "Intelligent Multiagent Control System for Energy and Comfort Management in Smart and Sustainable Buildings," in IEEE Transactions on Smart Grid, vol. 3, no. 2, pp. 605-617, June 2012.

[5] A. Khare and S. Rangnekar, "Optimal sizing of a grid integrated solar photovoltaic system," in IET Renewable Power Generation, vol. 8, no. 1, pp. 67-75, January 2014.

[6] M. Alsayed, M. Cacciato, G. Scarcella and G. Scelba, "Multicriteria Optimal Sizing of Photovoltaic-Wind Turbine Grid Connected Systems," in IEEE Transactions on Energy Conversion, vol. 28, no. 2, pp. 370-379, June 2013.

[7] Q. Li and M Zhou, “Research on Dependable Distributed Systems for Smart Grid,” Journal of Software, vol. 7, no.6, pp. 1250-1257, Jun. 2012.

[8] E. Babaci and O. Abbasi, "Structure for multi-input multi-output dc–dc boost converter," in IET Power Electronics, vol. 9, no. 1, pp. 9-19, 1 20 2016.

[9] C. Yaow-Ming, L. Yuan-Chuan, and W. Feng-Yu, "Mu lti-input dc/dc converter based on the multiwinding transformer for renewable energy applications," Industry Applications, IEEE Transactions on, vol. 38, no. 4, pp. l096-1104,2002.

[10] C. Huang-Jen, H. Hsiu-Ming, L. Li-Wei, and T. Ming-Hsiang, "A multiple-input dc/dc converter for renewable energy systems," in Industrial Technology, 2005. ICIT 2005. IEEE International Conference on,2005, pp.1304-1308.

[11] C. Yaow-Ming, L. Yuan-Chuan, H. Shih-Chieh, and C. Chung-Sheng, "Multi-input inverter for grid-connected hybrid pv/wind power system," Power Electronics, IEEE Transactions on, vol. 22, no. 3, pp. 1070-1077, 2007.

[12] H. Tao, A. Kotsopoulos, J. L. Duarte, and M. A. M. Hendrix, "Multiinput bidirectional dc-dc converter combining dc-link and magneticcoupling for fuel cell systems," in Industry Applications Conference, 2005. Fourtieth lAS Annual Meeting. Conference Record of the 2005, vol. 3, 2005, pp. 2021-2028 Vol. 3.

[13] Y. Yuan-mao and K. W. E. Cheng, "Multi-input voltage-summation converter based on switched-capacitor," Power Electronics, lET, vol. 6, no.9, pp.1909-1916,2013.

[14] J. Wei and B. Fahimi, "Multiport power electronic interface; concept, modeling, and design," Power

Electronics, IEEE Transactions on, vol. 26, no. 7, pp. 1890-1900,2011.
[15] L. Danwei and L. Hui, "A zvs bi-directional dc-dc converter for multiple energy storage elements," Power Electronics, IEEE Transactions on, vol. 21, no. 5, pp. 1513-1517,2006.
[16] T. Haimin, J. L. Duarte, and M. A. M. Hendrix, "Three-port triplehaif: bridge bidirectional converter with zero-voltage switching," Power Electronics, IEEE Transactions on, vol. 23, no. 2, pp. 782-792,2008.
[17] M. Delshad, A. T. Harchegani, M. Karimi and M. Mahdavi, "A new ZVT Multi Input Converter for hybrid sources systems," 2016 International Conference on Applied Electronics (AE), Pilsen, 2016, pp. 61-64.
[18] Yuanbin Li, Peng Ge and Ben Niu "Research on a Novel Soft-Switching Buck Converter," Research Journal of Applied Sciences, Engineering and Technology vol. 18, no. 5, pp. 4510-4517, May 2013.
[19] E. Adib and H. Farzanehfard, "New zero voltage transition PWM converters," inProc. IEEE ICIT Conf., 2006, pp. 801–806.
[20] G. Hua, E. X. Yang, Y. Jiang, and F. C. Lee, "Novel zero-current-transition PWM converters," IEEE Trans. Power Electron., vol. 9, pp. 601–606, Nov. 1994.
[21] J. G. Kassakian, M. F. Schlecht, and G. C. Verghese, "Principles of Power Electronics," Reading,MA: Addison-Wesley, 1991.
[22] E. Adib H. Farzanehfard, "Family of zero current zero voltage transition PWM converters," IET Power Electron (IREE)., Vol. 1, no. 2, pp. 214–223, 2008.
[23] S.H. Park,G.R. Cha, Y.C. Jung and C.Y. Won, "Design and application for PV generation system using a soft switching boost converter with SARC," IEEE Trans. On Industrial Electronics, vol. 57, no. 2, pp515-522, 2010.
[24] M. Mahdavi, H. Farzanehfard, "Zero-Current-Transition Bridgeless PFC Without Extra Voltage and Current Stress", in IEEE Trans. Ind. Electron., 2009, PP.2540-2547.
[25] M. Mahdavi, H. Farzanehfard, "A New Zero Voltage Transition Bridgeless PFC With Reduce conduction losses", Journal of Power Electronics, Vol. 9, No. 5, Sep 2009 PP.708-717.
[26] F. Marvi, E. Adib and H. Farzanehfard, "Zero voltage switching interleaved coupled inductor synchronous buck converter operating at boundary condition," in IET Power Electronics, vol. 9, no. 1, pp. 126-131,
[27] H. Choi, M. Jang and V. G. Agelidis, "Zero-current-switching bidirectional interleaved switched-capacitor DC–DC converter: analysis, design and implementation," in IET Power Electronics, vol. 9, no. 5, pp.
[28] P. Devender and, G. Parvathi, "A ZVS Dual-Input Converter With Hybrid Power Surces," in International Conference on Emerging Trends in Engineering & Technology (ICETET-2014) 29th - 30th September.
[29] R. J. Wai, C. Y. Lin, J. J. Liaw and Y. R. Chang, "Newly Designed ZVS Multi-Input Converter," in IEEE Transactions on Industrial Electronics, vol. 58, no. 2, pp. 555-566, Feb. 2011.
[30] R. W. Erickson, D. Maksimovix, Fundamentals of Power Electronics, 2nd Ed. pp 22- 27, 2001
[31] A. Di Napoli, F. Crescimbini, F. G. Capponi, and L. Solero, "Control strategy for multiple input DC–DC power converters devoted to hybrid vehicle propulsion systems," in Proc. IEEE ISIE 2002, pp. 1036–1041.

Amir Torki Harchegani was born in Shahrekord, Iran. He received his B.S. degree in Power Electrical Engineering from the Boroujen Branch, Islamic Azad University, Boroujen, Iran, in 2013; and his M.S. degree in Power Electrical Engineering from the Isfahan (Khorasgan) Branch, Islamic Azad University, Isfahan, Iran, in 2015. His current research interest include soft switching techniques.

Mohammad Mahdavi was born in Isfahan, Iran, in 1984. He received his B.S., M.S. and Ph.D. degrees in Electrical Engineering from the Isfahan University of Technology, Isfahan, Iran, in 2006, 2009 and 2013, respectively. Since 2013, he has been a Faculty Member in the Department of Electrical Engineering, Isfahan (Khorasgan) Branch, Islamic Azad University, Isfahan, Iran, where he is presently working as an Assistant Professor. He is the author of more than 25 technical papers published in journals and conference proceedings. His current research interests include high-frequency soft-switching converters, pulsed power applications, power factor correction, active power filters, and high- frequency electronic ballasts.

.